Redox-Active Carbohydrate-Coated Nanoparticles: Self-Assembly of a Cyclodextrin–Polystyrene Glycopolymer with Tetrazine–Naphthalimide

Andrew Gross, Raoudha Haddad, Christophe Travelet, Eric Reynaud, Pierre Audebert, Redouane Borsali, Serge Cosnier

LANGMUIR

Article

pubs.acs.org/Langmuir

Redox-Active Carbohydrate-Coated Nanoparticles: Self-Assembly of a Cyclodextrin–Polystyrene Glycopolymer with Tetrazine–Naphthalimide

Andrew J. Gross,[†] Raoudha Haddad,[†] Christophe Travelet,[‡,§] Eric Reynaud,[‡,§] Pierre Audebert,[∥] Redouane Borsali,*[,‡,§] and Serge Cosnier*[,†]

[†]Department of Molecular Chemistry, CNRS UMR 5250 and [‡]CERMAV, Université Grenoble Alpes, 38000 Grenoble, France

[§]CNRS, CERMAV, 38000 Grenoble, France

[∥]PPSM, CNRS UMR 8531, ENS Cachan, 61 Avenue du Président Wilson, 94235 Cachan, France

Supporting Information

ABSTRACT: The controlled self-assembly of precise and well-defined photochemically and electrochemically active carbohydrate-coated nanoparticles offers the exciting prospect of biocompatible catalysts for energy storage/conversion and biolabeling applications. Here an aqueous nanoparticle system has been developed with a versatile outer layer for host–guest molecule encapsulation via β-cyclodextrin inclusion complexes. A β-cyclodextrin-modified polystyrene polymer was first obtained by copper nanopowder click chemistry. The glycopolymer enables self-assembly and controlled encapsulation of tetrazine-naphthalimide, as a model redox-active agent, into nanoparticles via nanoprecipitation. Cyclodextrin host–guest interactions permit encapsulation and internanoparticle cross-linking for the formation of fluorescent compounds and clustered self-assemblies with chemically reversible electroactivity in aqueous solution. Light scattering experiments revealed stable particles with hydrodynamic diameters of 138 and 654 nm for nanoparticles prepared with tetrazine, of which 95% of the nanoparticles represent the smaller objects by number. Dynamic light scattering revealed differences as a function of preparation method in terms of size, 3-month stability, polydispersity, radius of gyration, and shape factor. Individual self-assemblies were visualized by atomic force microscopy and fluorescence microscopy and monitored in real-time by nanoparticle tracking analysis. UV–vis and fluorescence spectra provided insight into the optical properties and critical evidence for host–guest encapsulation as evidenced by solvachromatism and enhanced tetrazine uptake. Cyclic voltammetry was used to investigate the electrochemical properties and provided further support for encapsulation and an estimate of the tetrazine loading capacity in tandem with light scattering data.

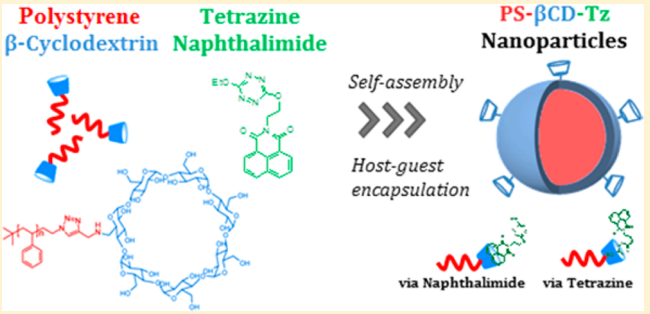

INTRODUCTION

The development of biocompatible nanoassembled particles with controlled chemical and physical properties has attracted significant attention for applications such as imaging, biosensing, drug delivery, and biocatalysis.[1,2] Nanoparticles such as micelles capable of carrying and delivering redox molecules in a selective manner have shown great benefits including enhanced bioavailability,[3] stimuli-responsiveness,[4] and reduced toxicity.[5] However, polymer synthesis and particle assembly methods are often complicated and time-consuming.[6] Furthermore, challenges remain for in vivo and in vitro applications including solubility and stability issues.

The preparation of amphiphilic glycopolymers provides a route to biocompatible and bioinspired nanoparticles but remains relatively undeveloped because of their tricky preparation with many synthesis steps.[7−9] Several groups have now reported on the preparation and self-assembly of block copolymers containing polysaccharides and oligosaccharides (maltoheptaose,[10] dextrans,[9,11] and amylose[12] with synthetic polymers such as polystyrenes,[9−13] poly(ε-caprolactone)s,[14] poly(ethylene glycol)s[15] and poly(methyl methacrylate)s[16]). Amphiphilic block copolymer formation is generally achieved using combinations of controlled living radical polymerizations, transition-metal-mediated coupling chemistry, and tedious purification procedures.[7] Many methods report the self-assembly of amphiphilic block copolymers into nanoparticles by direct dissolution into a selective solvent for one of the block moieties.[9,11,17,18] However, with this approach it is difficult to avoid random aggregation and control particle size at the nanoscale. Clever manipulation strategies involving indirect dissolution methods such as nanoprecipitation facilitate the preparation of well-defined micellar nanoparticles with

Received: September 25, 2016
Revised: October 20, 2016
Published: October 25, 2016

DOI: 10.1021/acs.langmuir.6b03512
Langmuir XXXX, XXX, XXX−XXX

narrow polydispersities from water or mixed solvent−water copolymer solutions.[13,16,19] Nanoprecipitation, first reported by Fessi and co-workers, involves the dissolution of both blocks followed by precipitation and selective solvent removal.[20,21] A further advantage is that redox molecules or drugs can be dissolved in copolymer solution prior to precipitation. In this case, hydrophobic species can be trapped as cargo inside the dense hydrophobic core of nanoassembled particles.[10,22]

A more sophisticated approach to encapsulation is to incorporate chemical handles capable not only of trapping but also of orienting and stimuli-controlled releasing of redox molecules in aqueous solution.[23] Methods capable of molecule encapsulation in the outer layer may further benefit from improved redox molecule bioavailability and accessibility. Cyclodextrins are one class of functional molecules capable of selectively binding a vast array of compounds via host−guest interactions.[24−27] Their low solubility in water leads to spontaneous aggregation, but functionalized cyclodextrins with carefully designed polymer blocks have been used to prepare nanoassembled particles.[7,9,13]

In this article, we describe a new straightforward synthesis route for the synthesis of a β-cyclodextrin-modified polystyrene polymer (PS-CD) and its use in the self-assembly of redox-active nanoparticles in water via encapsulation of a model hydrophobic molecule, tetrazine-naphthalimide (Tz). This molecule was recently developed by us and is of interest for future applications in fluorescence sensing and labeling.[28,29]

The PS-CD glycopolymer was synthesized according to a simple procedure that uses a copper nanopowder catalyst rather than copper in solution to covalently couple functionalized β-cyclodextrin and polystyrene blocks via click chemistry with a high yield of 90%. (See the Supporting Information for synthesis and characterization details.) We previously used CuI to couple β-cyclodextrin and PS groups, but the Cu in solution was difficult to remove so it was not possible to synthesize a large amount of clean glycopolymer.[13] In contrast, the Cu nanopowder employed here is very easy to remove via classical filtration and CupriSorb resin, facilitating preparation and purification of the modified polymer on a larger scale.

EXPERIMENTAL SECTION

General Materials and Apparatus. The ω-hydroxy-polystyrene (M_n = 3800 g mol^{-1}) was purchased from Polymer Source. Tetrazine-naphthalimide was synthesized according to our previously reported work.[29] Propargylamine, sodium hydroxide (NaOH), tetrahydrofuran (THF), *N*,*N*-dimethylformamide (DMF), sodium azide (NaN_3), and diatomaceous earth were purchased from Sigma-Aldrich. β-Cyclodextrin and Cu/CuO nanopowder were purchased from Alfa Aesar. Tosyl chloride (TsCl) was obtained from Fluka, and pyridine was purchased at SDS. Methanol (MeOH) and dichloromethane (CH_2Cl_2) were purchased from Biosolve. Milli-Q water was obtained by water purification to a resistivity of 18.2 MΩ cm using a Millipore Ultrapure system. Deuterated solvents were purchased from Eurisotop, the Cuprisorb resin was purchased from Seachem, and the Si(100) wafers were purchased from Siltronix. All reagents and solvents used for the synthesis of tetrazine-naphthalimide were purchased from Sigma-Aldrich or Carlo-Erba.

^{1}H NMR spectra were recorded on a Bruker Avance 400 MHz spectrometer with a frequency of 400.13 MHz and calibrated with the deuterated solvent signal.[30] The analysis characteristics were zg = 90°, D1 = 1 s, and NS = 128 scans. Matrix-assisted laser desorption ionization time-of-flight mass spectrometry (MALDI-TOF-MS) was performed using an Applied Biosystems Voyager-DE STR-H equipped with a nitrogen laser (337 nm and 3 ns pulse width).

UV−vis absorption spectra were recorded in quartz cuvettes using a PerkinElmer UV-Lambda 650 spectrophotometer, and fluorescence spectra were recorded using a PerkinElmer LS50.

Synthesis of β-Cyclodextrin-Modified Polystyrene Polymer. The amphiphilic glycopolymer was obtained by click chemistry. The first step was to functionalize each block: the hydrophobic block, ω-hydroxyl-terminated polystyrene, was functionalized to form ω-azido-terminated polystyrene via the ω-tosyl terminated polystyrene intermediate with an overall yield of 75% according to the method of Fallais and co-workers.[31] The hydrophilic block, native β-cyclodextrin, was monofunctionalized into mono-6-alkyne-β-cyclodextrin via the mono-6-tosyl-β-cyclodextrin intermediate with an overall yield of 7% according to the procedure developed by Moutard.[32,33] Both blocks with their complementary chemical functions (alkyne and azido) were subsequently linked together via a click reaction in heterogeneous media catalyzed by Cu nanopowder[34,35] to obtain the β-cyclodextrin-modified polystyrene polymer (M_n = 4900 g mol^{-1}, PDI = 1.01) (Scheme S1). To perform the click reaction, a degassed solution containing the azido-functionalized polystyrene (1 equiv, 8.1 g, 1.8 × 10^{-3} mol) and the alkynyl-functionalized cyclodextrin (1.2 equiv, 2.7 g, 2.2 × 10^{-3} mol) in DMF was first prepared. An excess of Cu nanopowder (1.8 equiv, 260 mg, 3.2 × 10^{-3} mol) was added to the solution and the mixture stirred under Ar at 65 °C for several hours until the azide ^{1}H NMR signal disappeared. At the end of the reaction, the crude heterogeneous mixture was filtered off under diatomaceous earth, and the obtained filtrate was stirred several hours in the presence of the Cuprisorb resin. The mixture was finally precipitated in cold MeOH to give a white powder with a yield of 90% (mass = 8 g). The modified polymer structure was confirmed using NMR and MALDI analysis (Figure S1).

Preparation of PS-CD$_{NP}$ and PS-CD-Tz$_{NP}$ Nanoparticles via Nanoprecipitation. Polymer solutions were prepared by dissolving either 5 mg of PS-CD or 5 mg of PS-CD together with 1 mg of tetrazine in 5 g of a THF/H_2O solution (80:20 v/v %, unless otherwise stated). For nanoprecipitation by method A, 1 g of the PS-CD solution was slowly added dropwise to 40 g of Milli-Q water under stirring at 500 rpm at room temperature. For nanoprecipitation by method B, 40 g of water was slowly added to 1 g of the PS-CD solution under stirring at 500 rpm at room temperature. The solutions were subsequently stirred at 500 rpm at room temperature for 1.5 h and then preconcentrated to 4 g by evaporation under reduced pressure at 50 °C using a rotary evaporator. The nanoparticle suspensions were stored at room temperature in the dark.

Static Light Scattering (SLS)/Dynamic Light Scattering (DLS). Light scattering measurements were performed using an ALV/CGS-8FS/N069 goniometer with an ALV/LSE-5004 multiple-τ digital corrector with a 125 ns initial sampling time and a 35 mW red HeNe linearly polarized laser operating at λ = 632.8 nm. Nanoparticle suspensions were loaded into 10-mm-diameter quartz cells thermostated at 25 ± 0.1 °C. Data were collected using the digital ALV correlator control software at observation angles relative to the transmitted beam of 90/150° (scattering vector moduli 1.87 × 10^{-2}/2.56 × 10^{-2} nm^{-1}) for a counting time of typically 180 s. In DLS measurements, relaxation time distributions were determined using a Contin analysis of the autocorrelation functions. Polydispersity values were calculated from the cumulant analysis of the DLS autocorrelations ($g^{(2)} - 1$).

Diffusion coefficients were obtained from eq 1 where D is the diffusion coefficient, τ is the relaxation time, and q is the modulus of the scattering vector:

$$D = \frac{1}{\tau q^2} \quad (1)$$

Hydrodynamic diameters, D_h, were calculated using the Stokes−Einstein equation (eq 2), where K_B is the Boltzmann constant, T is the temperature, η is the medium viscosity, and D is the diffusion coefficient:

$$D_h = \frac{K_B T}{3\pi\eta D} \quad (2)$$

DOI: 10.1021/acs.langmuir.6b03512
Langmuir XXXX, XXX, XXX−XXX

The percentage of small nanoparticles was calculated using eq 3, assuming that the nanoparticles behave like hard spheres in water and have the same density, where N_{small} refers to the number of small nanoparticles (fast relaxation mode), τ_{small} is the relaxation time corresponding to the small nanoparticles, and S_{small} is the surface area under the peak related to the small nanoparticles:[36]

$$\frac{N_{small}}{N_{big}} = \left(\frac{\tau_{big}}{\tau_{small}}\right)^3 \left(\frac{S_{small}}{S_{big}}\right) \quad (3)$$

For SLS measurements, scattering intensities were corrected by the background solvent signal. The diameter of gyration, D_g, was determined from eq 4, where n is the number of repetitive units and b is the Kuhn length:

$$D_g = 2\left(\frac{nb^2}{6}\right)^{0.5} \quad (4)$$

Electrochemistry. Electrochemical measurements were performed at room temperature using an Eco Chemie Autolab PGSTAT 100 potentiostat running GPES 4.9 software. A conventional three-electrode cell setup was used for all electrochemical experiments comprising a glassy carbon working electrode (GC, 3 mm diameter), a saturated calomel reference electrode (SCE), and a Pt wire counter electrode. The concentration of tetrazine-naphthalimide was estimated according to the Randles–Sevcik equation (eq 5) where I_p is the peak current, n is the number of electrons transferred in the redox event, F is the Faraday constant, C is the concentration of electroactive species, D is the diffusion coefficient (here estimated from dynamic light scattering), A is the geometric electrode area, ν is the scan rate, R is the gas constant, and T is room temperature:

$$I_p = nFAC\left(\frac{nF\nu D}{RT}\right)^{0.5} \quad (5)$$

Nanoparticle Tracking Analysis (NTA). NTA was carried out using a Nanosight LM10HS optical microscope setup equipped with a blue-purple laser (λ_{ex} = 405 nm), a camera, and a chamber mounted on a modified microscope stage (Nanosight, Amesbury, U.K.). The original suspensions of nanoparticles were diluted with Milli-Q water and introduced into the chamber with a syringe. Video clips of the nanoparticles subjected to their natural Brownian motion were captured over 60 s at 25.0 °C and analyzed using analytical software version 2.1, giving access to the number-weighted size distributions. (See the Supporting Information for 10 s video clips.)

Atomic Force Microscopy (AFM). Twenty microliters of a nanoparticle suspension was dropped onto a Si(100) substrate, and the sample was left to dry at room temperature overnight in a desiccator. AFM measurements were performed using a Dimension Icon (Bruker, Santa Barbara, CA) with SCANASIST-Air (Bruker, Santa Barbara, CA) probes in peak-force mode with a scan rate of 1 Hz. The data was processed using Gwyddion 2.41 microscope software.

Fluorescence Microscopy. Twenty microliters of a nanoparticle suspension was dropped onto a Si(100) substrate, and the sample was left to dry at room temperature overnight in a desiccator. Fluorescence microscopy images were recorded using an Olympus BX61 microscope coupled with an Olympus DP30BW camera and CellP imaging software. A DAPI (4′,6-diamidino-2-phenylindole) filter set was used: DAPI with λ_{ex} = 340–380 nm and λ_{em} = 450–490 nm. Images were recorded with an exposure time of 500 ms.

RESULTS AND DISCUSSION

For the preparation of nanoparticles in aqueous solution via nanoprecipitation, we focused our initial studies on optimizing the solvent system for both blocks of the PS-CD glycopolymer. Tetrahydrofuran was chosen as the organic solvent because of its good solubility toward polystyrenes and Tz, water miscibility, and good evaporation rate. Static light scattering experiments were recorded for a series of PS-CD solutions prepared in THF with water content of between 0 and 50% (Figure S2). Very low scattering intensities were observed in the presence of 5 to 20% water, consistent with desirable polymer chain dissolution and few aggregates in a mixed solvent. In the presence of ≥20% water, a significant increase in scattering intensity was observed because of the unwanted formation of self-assemblies. β-Cyclodextrin-modified polymer solutions were therefore investigated in 10 and 20% water solutions. However, further observations proved that suspensions based on 10% water solutions were more unstable, with microscopic particles visible after just a few days of storage, and thus the 80:20 THF/water ratio was adopted for further investigations.

We explored the controlled self-assembly of PS-CD (1 mg g^{-1}) in the presence and absence of Tz (0.2 mg g^{-1}) in THF/H_2O via nanoprecipitation in a large excess of water (Figure 1A). For the PS-CD with Tz solution, the PS-CD/Tz mole-to-mole ratio used was 1:3. Herein, suspensions obtained from PS-CD and PS-CD with Tz will be referred to as PS-CD_{NP} and PS-CD-Tz_{NP}, respectively. Two methods of nanoprecipitation were explored: method A, where 1 g of PS-CD polymer solution was slowly added to 40 g of water (solvent-to-water method), and method B, where 40 g of water was slowly added to 1 g of PS-CD polymer solution (water-to-solvent method). For both methods A and B, the same precipitation and evaporation procedures were performed (Experimental Section) to obtain aqueous PS-CD_{NP} and PS-CD-Tz_{NP} suspensions.

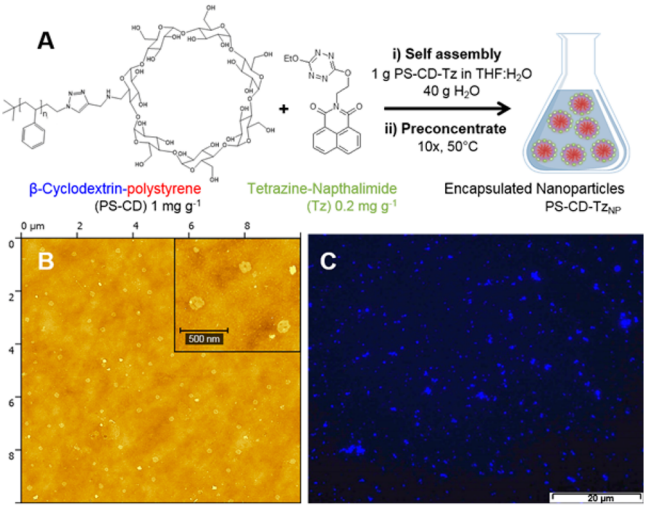

Figure 1. (A) Synthesis route for the preparation of encapsulated nanoparticles (PS-CD-Tz_{NP}). (B, C) Images of PS-CD-Tz_{NP} particles prepared by method A on silicon recorded by (B) AFM in peak-force mode at 1 Hz and (C) fluorescence microscopy with a DAPI filter and a 500 ms exposure time.

The ability of the β-cyclodextrin-modified polystyrene solutions to spontaneously assemble into nanoparticles was initially confirmed by atomic force microscopy and fluorescence microscopy after solution drop-casting and drying on a silicon wafer (Figure 1B,C). AFM imaging of the PS-CD-Tz_{NP} sample prepared by method A revealed the presence of individual nanoparticles with an average particle diameter of 167 ± 30 nm (n = 89 particles). Importantly, the brief AFM analysis proved the successful formation of nanoparticle self-assemblies using our nanoprecipitation protocol. Figure 1C shows a fluorescence

DOI: 10.1021/acs.langmuir.6b03512
Langmuir XXXX, XXX, XXX–XXX

microscopy image of the PS-CD-Tz_{NP} sample recorded with a DAPI filter at λ_{ex} = 340−380 nm and λ_{em} = 450−490 nm. Bright fluorescence over a long lifetime using a DAPI filter was observed from the particles on the surface. In contrast, insignificant fluorescence was observed for PS-CD_{NP} (data not shown), consistent with the successful encapsulation of the small organic tetrazine-containing bifluorophore in PS-CD-Tz_{NP} particles.[28]

Dynamic light scattering experiments were performed to examine the suspensions in more detail. Initial DLS was performed on PS-CD_{NP} (Figure 2A) and PS-CD-Tz_{NP} (Figure 2B) prepared by methods A and B to optimize the nanoprecipitation protocol for the preparation of well-defined nanoassemblies.

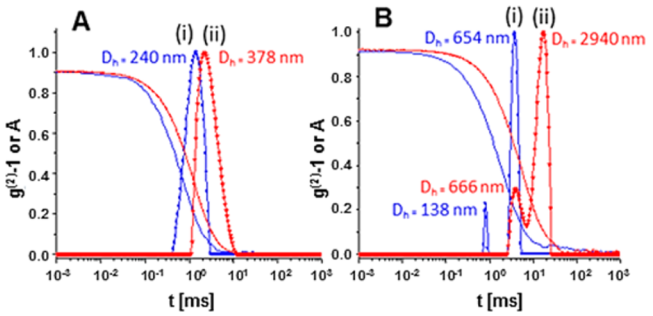

Figure 2. DLS autocorrelation ($g^{(2)}$ − 1) measured at 90° and relaxation time distribution of aqueous suspensions of (A) PS-CD_{NP} prepared by (i) method A and (ii) method B and (B) PS-CD-Tz_{NP} prepared by (i) method A and (ii) method B.

Figure 2A shows the DLS autocorrelation function ($g^{(2)}$ − 1) and relaxation time distribution for the PS-CD_{NP} suspensions. For PS-CD_{NP} prepared by methods A (Figure 2Ai) and B (Figure 2Aii), unimodal distributions of relaxation times were observed corresponding to mean hydrodynamic diameters of D_h = 240 and 378 nm with polydispersities of $Đ$ = 1.34 and 1.45, respectively. The particles prepared by method A are therefore smaller and less polydisperse than those prepared by method B. The PS-CD_{NP} particles prepared by method A are comparable in size to previously reported compound micelles with D_h ≈ 160 nm prepared by the self-assembly of polystyrene-containing diblock polymers.[10,15] Figure 2B shows the DLS autocorrelation function ($g^{(2)}$ − 1) and relaxation time distribution for the PS-CD-Tz_{NP} suspensions prepared by methods A (Figure 2Bi) and B (Figure 2Bii). The relaxation time distribution plots, reflecting mass-weighted distributions, show the appearance of two particle sizes for PS-CD-Tz_{NP}. The PS-CD-Tz_{NP} suspension obtained by method B exhibits greater polydispersity ($Đ$ = 1.43) and contains microscale particles (D_h = 2940 nm). In contrast, smaller nanoparticles with a lower polydispersity ($Đ$ = 1.32) are obtained by method A, and thus this method of nanoprecipitation was adopted for further analysis.

The smaller particle size of D_h = 138 nm observed for PS-CD-Tz_{NP} prepared by method A is attributed to small self-assemblies that have decreased in size compared to the PS-CD_{NP} nanoparticles prepared by the same method as a result of the encapsulation of Tz molecules and the shrinking of the more hydrophobic core. A change in self-assembly behavior of the PS-CD polymer in the presence of Tz was expected because the cone-shaped hydrophobic cavities of the β-cyclodextrin groups drive the 1:1 inclusion of guest Tz molecules via 1,8-naphthalimide (equatorial inclusion) and 1,2,4,5-tetrazine groups.[29,37] A decrease in size with encapsulation has previously been reported for self-assembled nanoparticles with encapsulated hydrophobic molecules.[15] The larger nanoparticles of PS-CD-Tz_{NP} with D_h = 654 nm, observed only after self-assembly in the presence of Tz, are attributed to nanoparticle clusters. The formation of clusters is attributed to the cross-linking of individual particles via host−guest interactions between Tz molecules and host β-cyclodextrin groups located at the periphery of the particles. (Both tetrazine and naphthalimide functional groups can function as guests.) Particle aggregation due to nonspecific interactions[3] must be considered and likely contributes to the self-assembly of the larger particle distribution. Regardless of the nature of formation of the larger particles, their presence in terms of number is very small compared to the smaller particles. On the basis of 12 DLS measurements at 90°, the estimated number of smaller objects is 95.1% ($N_{small} \approx 19.1 N_{big}$), according to eq 3.

To complete the nanoparticle sizing experiments, nanoparticle tracking analysis was performed. Nanoparticles were illuminated with a 405 nm blue laser and tracked individually (Figure 3, Figure S3 and corresponding video clips in the Supporting Information). Nanoparticles that undergo Brownian motion were taken into account, and average $D_{h,NTA}$ values of 195 nm for PS-CD_{NP} and 105 nm for PS-CD-Tz_{NP} were acquired. These values are smaller than those obtained by DLS because of the fact that number-weighted distributions are obtained. Nevertheless, the sizes obtained by NTA are complementary, with the corresponding particle sizes obtained by DLS (D_h = 240 and 138 nm). The absence of the larger cluster distribution for PS-CD-Tz_{NP} by NTA is not at all surprising given that (i) NTA gives access to number-weighted distributions of which only ∼4.9% are the clusters and (ii) only a few nanoparticles are imaged, as can be seen in Figure S3 and the video clips.

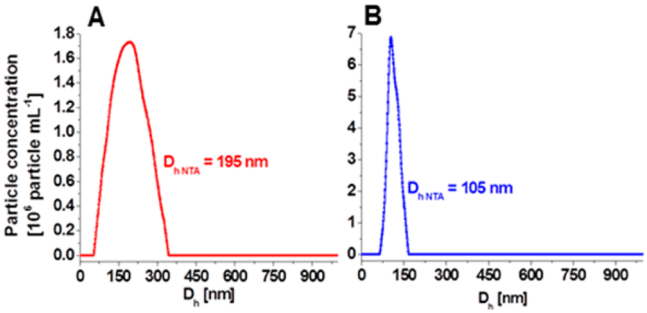

Figure 3. Hydrodynamic number-weighted size distributions by NTA of (A) PS-CD_{NP} and (B) PS-CD-Tz_{NP} suspensions prepared by method A.

Further analysis of the DLS and SLS scattering data was performed to shed light on the shape of the nanoparticles. First, the diameter of gyration, D_g, was determined from SLS angular dependence experiments via Guinier plots (Figure 4). Values of D_g = 326 and 258 nm were obtained from the slope of the linear fit in the low qD_g region for PS-CD_{NP} and PS-CD-Tz_{NP}, respectively. Next, the shape factor, ρ, was obtained from the ratio $\rho = D_g/D_h$, as proposed by Burchard.[38] The ρ values of 1.4 for PS-CD_{NP} and 1.9 for PS-CD-Tz_{NP} fall between those of vesicles (ρ = 1) and rigid rods ($\rho \geq 2.0$), and thus PS-CD_{NP} and PS-CD-Tz_{NP} particles can be ascribed to particles whose

DOI: 10.1021/acs.langmuir.6b03512
Langmuir XXXX, XXX, XXX−XXX

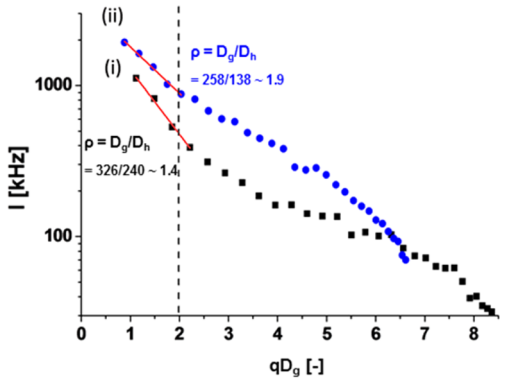

Figure 4. SLS Guinier plots of the scattering intensity of (i) PS-CD_{NP} and (ii) PS-CD-Tz_{NP} suspensions prepared by method A.

overall shape is spherical (1.4) and polydisperse spheres (1.9), respectively.[38]

An important issue largely overlooked in previous studies on the self-assembly of saccharide-based polymers is their stability. In this study, we tested the long-term stability of PS-CD_{NP} and PS-CD-Tz_{NP} suspensions by monitoring the particle size change after storage in the dark at ambient temperature for 3 months. The DLS data (Figure S4) reveal relatively small increases in hydrodynamic radii for PS-CD-Tz_{NP} compared to markedly larger increases in radii for PS-CD_{NP} particles. The apparent low stability of the nonencapsulated PS-CDNP particles is attributed to nonspecific hydrophobic interactions of β-cyclodextrin groups at the periphery of the nanoparticles, which give larger aggregations over time. The higher stability of PS-CD-Tz_{NP} reflects the saturation of these β-cyclodextrin groups, which in turn suppresses particle aggregation over time. Crucially, the stability of PS-CD-Tz_{NP} suggests little evidence of the presence of Tz molecules in solution that would likely increase particle aggregation.

UV−vis and fluorescence spectra were recorded to probe the ability of the PS-CD polymer to encapsulate tetrazine-naphthalimide during self-assembly. Three solutions were investigated: as-prepared PS-CD_{NP}, PS-CD-Tz_{NP} (Tz = 0.06 mg mL^{-1}), and a saturated tetrazine-naphthalimide in water solution (H_2O-Tz) prepared by addition of 0.3 mg Tz in 3 mL (Tz < 0.1 mg mL^{-1}). The absorption spectrum for PS-CD_{NP} in the absence of Tz shows weak background absorption due to the polymer but no well-defined absorption peaks (Figure 5Ai). In contrast, both PS-CD-Tz_{NP} (Figure 5Aii) and H_2O-Tz (Figure 5Aiii) solutions exhibit a strong absorption band at 340−380 nm, ascribed to both the imide group and the $\pi-\pi^*$ band transition of the tetrazine group. Significantly larger absorption is observed for PS-CD-Tz_{NP} compared to the H_2O-Tz, consistent with improved solubilization of the Tz via host−guest encapsulation. The small hypsochromic shift (blue shift) from λ_{max} = 353 nm for H_2O-Tz to 341 nm for PS-CD-Tz_{NP} is consistent with the Tz molecules shifting from a polar to a nonpolar environment. The shift therefore provides further evidence of the inclusion of Tz in the hydrophobic β-cyclodextrin cavities. Such small blue shifts in UV−vis spectra due to host−guest complexation have previously been reported for 4-amino-1,8-naphthalimides with β-cyclodextrin molecules.[37] Another remarkable feature of the fluorescence emission of the encapsulated molecules is that both the imide antenna and the tetrazine acceptor emit together (producing almost white light), proving that the energy transfer is partially

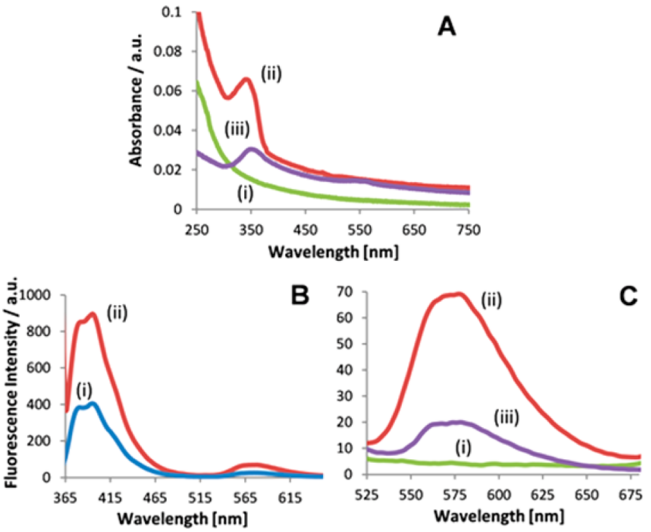

Figure 5. (A) UV−vis absorption spectra for (i) PS-CD_{NP}, (ii) PS-CD-Tz_{NP}, and (iii) H_2O-Tz. (B, C) Fluorescence emission spectra recorded at λ_{ex} = 353 nm for (B) PS-CD-Tz_{NP} at 365 to 650 nm and (C) (i) PS-CD_{NP}, (ii) PS-CD-Tz_{NP}, and (iii) H_2O-Tz at 525 to 680 nm.

blocked as a consequence of the encapsulation process. This is in sharp contrast to the situation encountered when the molecules are dissolved in an organic solvent, where the energy transfer occurs with a ca. 90% efficiency and only tetrazine fluorescence is observed.[28]

Fluorescence spectra of PS-CD-Tz_{NP} nanoparticles were initially recorded at different emission wavelengths. Strong fluorescence was observed only upon excitation in the UV region at λ_{ex} = 353 nm (Figure 5B) and λ_{ex} = 340 nm (data not shown) and not at higher wavelengths (for example, λ_{ex} = 518 and 544 nm, data not shown). The classical strong fluorescence of 1,8-naphthalimide was observed between 370 and 420 nm along with a weak fluorescence band at 550−600 nm due to the tetrazine moiety. Further evidence for the improved uptake of fluorescent Tz molecules via molecular encapsulation was obtained by comparison of the fluorescence spectra recorded at λ_{ex} = 340 nm for PS-CD_{NP}, PS-CD-Tz_{NP}, and H_2O-Tz solutions (Figure 5C). No fluorescence was observed for nanoparticles free of Tz (Figure 5Ci), as expected. A clear enhancement in fluorescence was, however, observed at λ_{em} = 570 nm for PS-CD-Tz_{NP} (Figure 5Cii) compared to the Tz-saturated H_2O-Tz solution, reflecting the improved solubility of tetrazine-naphthalamide in the nanoparticle solution compared to water.

Cyclic voltammograms (CVs) of the solutions were also performed to test the electroactivity of the nanoparticles. CVs were recorded at glassy carbon electrodes without supporting electrolyte to avoid aggregation due to increased ionic strength. In the absence of Tz, a typical background response of a GC electrode in aqueous solution was observed (Figure 6Ai). For PS-CD-Tz_{NP} nanoparticles, a single well-defined and chemically reversible redox couple at $E_{1/2}$ = −0.32 V vs SCE was observed (Figure 6Aii). This system is attributed to a two-electron, two-proton reduction of 1,4-tetrazine to its protonated form, 1,4-dihydrotetrazine.[29,39] This behavior is analogous to the two-electron reduction of quinones to hydroquinones in aqueous solution. It should be noted that the CV recorded in H_2O-Tz solution (Figure S5i) shows an almost identical $E_{1/2}$ but with an extremely weak peak intensity, reflecting the trace presence of

DOI: 10.1021/acs.langmuir.6b03512
Langmuir XXXX, XXX, XXX−XXX

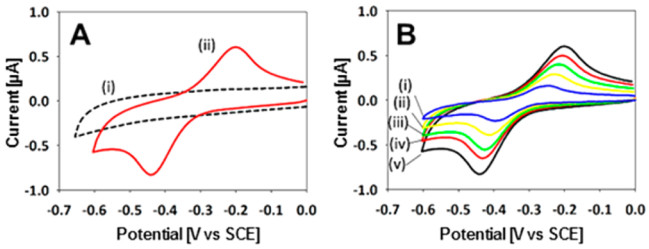

Figure 6. CVs recorded at glassy carbon on (A) (i) PS-CD_{NP} and (ii) PS-CD-Tz_{NP} at 100 mV s^{-1} and (B) PS-CD-Tz_{NP} at (i) 20, (ii) 40, (iii) 60, (iv) 80, and (v) 100 mV s^{-1}.

Tz for the Tz-saturated H_2O solution. However, the peak-to-peak separation for H_2O-Tz (ΔE_p = 149 mV) is smaller than that recorded for PS-CD-Tz_{NP}, suggesting slower apparent electron-transfer kinetics for the encapsulated nanoparticles. The latter may be assigned to a phenomenon of electron hopping between Tz molecules encapsulated within cyclodextrin groups located at the periphery and inside the poorly conducting polystyrene core. Thus, the tetrazine-containing nanoparticles are redox-active and electrochemically accessible, which has important implications for future catalytic and sensing applications.

Finally, CVs of the PS-CD-Tz_{NP} solution were recorded at scan rates in the range of 20 to 100 mV s^{-1}. A linear dependence between the peak current and the square root of the scan rate, indicative of diffusion-controlled behavior (Figure S6), was observed. Assuming diffusion-controlled behavior, we applied the Randles–Sevcik equation (eq 5) to estimate the average concentration of electroactive Tz molecules encapsulated in the nanoparticles, thus providing an idea of possible drug or redox molecule loading capacity. From the oxidative peak current shown in Figure 6A and using the diffusion coefficient obtained for the small particles of 3.57×10^{-8} cm^2 s^{-1} via DLS analysis using eq 1, the estimated Tz concentration for PS-CD-Tz_{NP} is 1.5×10^{-4} mol L^{-1}.

CONCLUSIONS

A new bioinspired β-cyclodextrin-modified polystyrene polymer has been prepared using a heterogeneous copper nanocatalyst that facilitates glycopolymer purification and preparation on a larger scale. Self-assembly via a "solvent-to-water" nanoprecipitation method, in the presence of tetrazine-naphthalimide, forms stable redox-active nanoassembled particles and clusters with mean hydrodynamic diameters of 138 and 654 nm, respectively. The nanoparticles are considered to be spheres constituting β-cyclodextrin and polystyrene blocks, with β-cyclodextrin groups present in the outer layer. Increased UV absorption, fluorescence, and electrochemical signals confirm both the presence and improved uptake of tetrazine-naphthalimide molecules in nanoparticles compared to water. Solvochromatic shifts and a slight decrease in electrochemical reversibility for the redox-active molecules in the nanoparticles are consistent with their encapsulation in the nanoparticles and their surface via Tz inclusion in β-cyclodextrin groups. Furthermore, the fluorescence emission reveals that both the imide antenna and tetrazine acceptor emit together, proving that the energy transfer between the chromophores is partially deactivated. As a consequence, the fluorescence emission is less brilliant than that observed for the tetrazine-naphthalimide dyad in organic solvent. The formation of a small number of large clusters, observed here only by light scattering experiments, is possible via a novel type of host–guest interparticle cross-linking where tetrazine-naphthalimide molecules act as a nanoparticle cross-linker. The potential use of the new glycopolymer for host–guest encapsulation of electrocatalysts for the construction of enzymatic biofuel cells with improved performance and biocompatibility is currently underway.

ASSOCIATED CONTENT

Supporting Information

The Supporting Information is available free of charge on the ACS Publications website at DOI: 10.1021/acs.langmuir.6b03512.

Glycopolymer synthesis details and characterization data by DLS, NTA, and voltammetry (PDF)

Nanoparticle tracking analysis of PS-CD and PS-CD-TzNP suspensions prepared by method A (ZIP)

AUTHOR INFORMATION

Corresponding Authors

*E-mail: borsali@cermav.cnrs.fr.

*E-mail: serge.cosnier@univ-grenoble-alpes.fr.

Notes

The authors declare no competing financial interest.

ACKNOWLEDGMENTS

This work was supported by LABEX ARCANE (ANR-11-LABX-0003-01) and platform Chimie NanoBio ICMG FR 2607 (PCN-ICMG). We gratefully acknowledge the assistance of Hugues Bonnet with AFM imaging.

REFERENCES

(1) Gaitzsch, J.; Huang, X.; Voit, B. Engineering Functional Polymer Capsules toward Smart Nanoreactors. *Chem. Rev.* **2016**, *116* (3), 1053–1093.

(2) Nicolas, J.; Mura, S.; Brambilla, D.; Mackiewicz, N.; Couvreur, P. Design, Functionalization Strategies and Biomedical Applications of Targeted Biodegradable/Biocompatible Polymer-Based Nanocarriers for Drug Delivery. *Chem. Soc. Rev.* **2013**, *42* (3), 1147–1235.

(3) Qu, X.; Khutoryanskiy, V. V.; Stewart, A.; Rahman, S.; Papahadjopoulos-Sternberg, B.; Dufes, C.; McCarthy, D.; Wilson, C. G.; Lyons, R.; Carter, K. C.; Schatzlein, A.; Uchegbu, I. F. Carbohydrate-Based Micelle Clusters which Enhance Hydrophobic Drug Bioavailability by up to 1 Order of Magnitude. *Biomacromolecules* **2006**, *7* (12), 3452–3459.

(4) Li, C. H.; Liu, S. Y. Polymeric Assemblies and Nanoparticles with Stimuli-Responsive Fluorescence Emission Characteristics. *Chem. Commun.* **2012**, *48* (27), 3262–3278.

(5) Farokhzad, O. C.; Cheng, J. J.; Teply, B. A.; Sherifi, I.; Jon, S.; Kantoff, P. W.; Richie, J. P.; Langer, R. Targeted Nanoparticle-Aptamer Bioconjugates for Cancer Chemotherapy in vivo. *Proc. Natl. Acad. Sci. U. S. A.* **2006**, *103* (16), 6315–6320.

(6) Meier, W. Polymer Nanocapsules. *Chem. Soc. Rev.* **2000**, *29* (5), 295–303.

(7) Xu, Z.; Liu, S.; Liu, H.; Yang, C.; Kang, Y.; Wang, M. Unimolecular Micelles of Amphiphilic Cyclodextrin-Core Star-like Block Copolymers for Anticancer Drug Delivery. *Chem. Commun.* **2015**, *51* (87), 15768–15771.

(8) Zhang, Y.; Hsu, B. Y. W.; Ren, C. L.; Li, X.; Wang, J. Silica-Based Nanocapsules: Synthesis, Structure Control and Biomedical Applications. *Chem. Soc. Rev.* **2015**, *44* (1), 315–335.

(9) Kakuchi, T.; Narumi, A.; Miura, Y.; Matsuya, S.; Sugimoto, N.; Satoh, T.; Kaga, H. Glycoconjugated Polymer. 4. Synthesis and Aggregation Property of Well-Defined End-Functionalized Polystyrene with β-Cyclodextrin. *Macromolecules* **2003**, *36* (11), 3909–3913.

DOI: 10.1021/acs.langmuir.6b03512
Langmuir XXXX, XXX, XXX–XXX

(10) Otsuka, I.; Osaka, M.; Sakai, Y.; Travelet, C.; Putaux, J.-L.; Borsali, R. Self-Assembly of Maltoheptaose-block-Polystyrene into Micellar Nanoparticles and Encapsulation of Gold Nanoparticles. *Langmuir* **2013**, *29* (49), 15224−15230.
(11) Houga, C.; Le Meins, J. F.; Borsali, R.; Taton, D.; Gnanou, Y. Synthesis of ATRP-Induced Dextran-b-Polystyrene Diblock Copolymers and Preliminary Investigation of their Self-Assembly in Water. *Chem. Commun.* **2007**, *29*, 3063−3065.
(12) Ouhib, R.; Renault, B.; Mouaziz, H.; Nouvel, C.; Dellacherie, E.; Six, J. L. Biodegradable Amylose-g-PLA Glycopolymers from Renewable Resources. *Carbohydr. Polym.* **2012**, *89* (1), 305−305.
(13) Giacomelli, C.; Schmidt, V.; Putaux, J. L.; Narumi, A.; Kakuchi, T.; Borsali, R. Aqueous Self-Assembly of Polystyrene Chains End-Functionalized with beta-Cyclodextrin. *Biomacromolecules* **2009**, *10* (2), 449−453.
(14) Suriano, F.; Coulembier, O.; Degee, P.; Dubois, P. Carbohydrate-based amphiphilic diblock copolymers: Synthesis, Characterization, and Aqueous Properties. *J. Polym. Sci., Part A: Polym. Chem.* **2008**, *46* (11), 3662−3672.
(15) He, Q.; Wu, W.; Xiu, K.; Zhang, Q.; Xu, F.; Li, J. Controlled Drug Release System Based on Cyclodextrin-Conjugated Poly(lactic acid)-b-Poly(ethylene glycol) Micelles. *Int. J. Pharm.* **2013**, *443* (1−2), 110−119.
(16) Zepon, K.; Otsuka, I.; Bouilhac, C.; Muniz, E. C.; Soldi, V.; Borsali, R. Self-assembly of Oligosaccharide-b-PMMA Block Copolymer Systems: Glyco-Nanoparticles and their Degradation under UV Exposure. *Langmuir* **2016**, *32* (18), 4538−4545.
(17) Cianga, L.; Bendrea, A.-D.; Fifere, N.; Nita, L. E.; Doroftei, F.; Ag, D.; Seleci, M.; Timur, S.; Cianga, I. Fluorescent Micellar Nanoparticles by Self-Assembly of Amphiphilic, Nonionic and Water Self-Dispersible Polythiophenes with "Hairy Rod" Architecture. *RSC Adv.* **2014**, *4* (99), 56385−56405.
(18) Xu, B.; Gu, G.; Feng, C.; Jiang, X.; Hu, J.; Lu, G.; Zhang, S.; Huang, X. (PAA-g-PS)-co-PPEGMEMA Asymmetric Polymer Brushes: Synthesis, Self-Assembly, and Encapsulating Capacity for both Hydrophobic and Hydrophilic Agents. *Polym. Chem.* **2016**, *7* (3), 613−624.
(19) Yin, L.; Dalsin, M. C.; Sizovs, A.; Reineke, T. M.; Hillmyer, M. A. Glucose-Functionalized, Serum-Stable Polymeric Micelles from the Combination of Anionic and RAFT Polymerizations. *Macromolecules* **2012**, *45* (10), 4322−4332.
(20) Fessi, H.; Devissaguet, J. P.; Puisieux, F.; Thies, C. Method of Formation of Colloidal Nanoparticles. FR 2,608,988 A1 1988.
(21) Fessi, H.; Puisieux, F.; Devissaguet, J. P.; Ammoury, N.; Benita, S. Nanocapsule Formation by Interfacial Polymer Deposition following Solvent Displacement. *Int. J. Pharm.* **1989**, *55* (1), R1−R4.
(22) Zepon, K. M.; Otsuka, I.; Bouilhac, C.; Muniz, E. C.; Soldi, V.; Borsali, R. Glyco-Nanoparticles Made from Self-Assembly of Maltoheptaose-block-Poly(methyl methacrylate): Micelle, Reverse Micelle, and Encapsulation. *Biomacromolecules* **2015**, *16* (7), 2012−2024.
(23) McLaughlin, C. K.; Logie, J.; Shoichet, M. S. Core and Corona Modifications for the Design of Polymeric Micelle Drug-Delivery Systems. *Isr. J. Chem.* **2013**, *53* (9−10), 670−679.
(24) Kang, Y.; Guo, K.; Li, B. J.; Zhang, S. Nanoassemblies Driven by Cyclodextrin-Based Inclusion Complexation. *Chem. Commun.* **2014**, *50* (76), 11083−11092.
(25) Stoffelen, C.; Huskens, J. Soft Supramolecular Nanoparticles by Noncovalent and Host-Guest Interactions. *Small* **2016**, *12* (1), 96−119.
(26) Guo, M.; Jiang, M.; Zhang, G. Surface Modification of Polymeric Vesicles via Host-Guest Inclusion Complexation. *Langmuir* **2008**, *24* (19), 10583−10586.
(27) Versluis, F.; Tomatsu, I.; Kehr, S.; Fregonese, C.; Tepper, A. W. J. W.; Stuart, M. C. A.; Ravoo, J.; Koning, R.; Kros, A. Shape and Release Control of a Peptide Decorated Vesicle through pH Sensitive Orthogonal Supramolecular Interactions. *J. Am. Chem. Soc.* **2009**, *131* (37), 13186−13187.
(28) Zhou, Q.; Audebert, P.; Clavier, G.; Meallet-Renault, R.; Miomandre, F.; Shaukat, Z.; Vu, T. T.; Tang, J. New Tetrazines Functionalized with Electrochemically and Optically Active Groups: Electrochemical and Photoluminescence Properties. *J. Phys. Chem. C* **2011**, *115* (44), 21899−21906.
(29) Fritea, L.; Audebert, P.; Galmiche, L.; Gorgy, K.; Le Goff, A.; Villalonga, R.; Săndulescu, R.; Cosnier, S. First Occurrence of Tetrazines in Aqueous Solution: Electrochemistry and Fluorescence. *ChemPhysChem* **2015**, *16* (17), 3695−3699.
(30) Fulmer, G. R.; Miller, A. J. M.; Sherden, N. H.; Gottlieb, H. E.; Nudelman, A.; Stoltz, B. M.; Bercaw, J. E.; Goldberg, K. I. NMR Chemical Shifts of Trace Impurities: Common Laboratory Solvents, Organics, and Gases in Deuterated Solvents Relevant to the Organometallic Chemist. *Organometallics* **2010**, *29* (9), 2176−2179.
(31) Fallais, I.; Devaux, J.; Jérôme, R. End-Capping of Polystyrene by Aliphatic Primary Amine by Derivatization of Precursor Hydroxyl End Group. *J. Polym. Sci., Part A: Polym. Chem.* **2000**, *38* (9), 1618−1629.
(32) Moutard, S.; Relation entre la Structure et les Propriétés d'Organisation de Nouvelles Cyclodextrines Amphiphiles. Ph.D. Thesis, Picardie Jules Verne University, France, 2003.
(33) Guo, Z.; Jin, Y.; Liang, T.; Liu, Y.; Xu, Q.; Liang, X.; Lei, A. Synthesis, Chromatographic Evaluation and Hydrophilic Interaction/Reversed-Phase Mixed-Mode Behavior of a "Click β-Cyclodextrin" Stationary Phase. *J. Chromatogr. A* **2009**, *1216* (2), 257−263.
(34) Elamari, H.; Etudes sur la Catalyse de la Reaction de Huisgen et Nouvelles Applications Synthetiques. Ph.D. Thesis, University Pierre and Marie Curie, France, 2013.
(35) Isaacman, M. J.; Barron, K. A.; Theogarajan, L. S. Clickable Amphiphilic Triblock Copolymers. *J. Polym. Sci., Part A: Polym. Chem.* **2012**, *50* (12), 2319−2329.
(36) Korchia, L.; Bouilhac, C.; Lapinte, V.; Travelet, C.; Borsali, R.; Robin, J.-J. Photodimerization as an Alternative to Photocrosslinking of Nanoparticles: Proof of Concept with Amphiphilic Linear Polyoxazoline Bearing Coumarin Unit. *Polym. Chem.* **2015**, *6* (33), 6029−6039.
(37) Brochsztain, S.; Rodrigues, M. A.; Politi, M. J. Inclusion Complexes of Naphthalimide Derivatives with Cyclodextrins. *J. Photochem. Photobiol., A* **1997**, *107* (1−3), 195−200.
(38) Walther, B. In *Polysaccharides: Structural Diversity and Functional Versatility*; Dumitriu, S., Ed.; CRC Press: New York, 2004; Chapter 7.
(39) Ehret, F.; Wu, H. X.; Alexander, S. C.; Devaraj, N. K. Electrochemical Control of Rapid Bioorthogonal Tetrazine Ligations for Selective Functionalization of Microelectrodes. *J. Am. Chem. Soc.* **2015**, *137* (28), 8876−8879.

DOI: 10.1021/acs.langmuir.6b03512
Langmuir XXXX, XXX, XXX−XXX